Electronic Supplementary Material (ESI) for Materials Chemistry Frontiers.

Electronic Supplementary Information

Synergistic effect of Sn doping and hydrogenation on hematite electrodes for photoelectrochemical water oxidation

Tae Hwa Jeon,[a,b] Hae-in Cho,[c] Hyunwoong Park,[d] Hyoung-il Kim,[c,e] and Wonyong Choi [a,f]**

[a] *Division of Environmental Science and Engineering, Pohang University of Science and Technology (POSTECH), Pohang 37673, Republic of Korea*
[b] *Department of Civil and Environmental Engineering, Rice University, Houston, TX 77005, USA*
[c] *Department of Civil and Environmental Engineering, Yonsei University, Seoul, 03722, Republic of Korea*
[d] *School of Energy Engineering, Kyungpook National University, Daegu 702-701, Korea*
[e] *Future City Open Innovation Center, Pohang University of Science and Technology (POSTECH), Pohang 37673, Korea.*
[f] *Institute for Convergence Research and Education in Advanced Technology, Yonsei University, Seoul 03722, Korea*

* To whom correspondence should be addressed (W. Choi & H.-I Kim)
E-mail for W.C.: wchoi@postech.edu, E-mail for H.-I K: hi.kim@yonsei.ac.kr

Table S1 ICP-MS analysis of $Sn\text{-}Fe_2O_3$ and $H\text{-}Sn\text{-}Fe_2O_3$.

Element	Fe		Sn	
	Concentration (μg/mL)	RSD[1] (%)	Concentration (μg/mL)	RSD (%)
$Sn\text{-}Fe_2O_3$	5.888	0.77	0.251	0.38
$H\text{-}Sn\text{-}Fe_2O_3$	6.366	1.30	0.240	1.73

[1]RSD: Relative Standard Deviation

Atomic% of Sn was estimated as follow:

The concentration of Fe and Sn in both samples was first converted to μmol/L based on molecular weight (55.845 and 118.71 g/mol for Fe and Sn, respectively).

For $Sn\text{-}Fe_2O_3$,

$$Sn(Atomic\%) = \frac{Sn(\mu mol/L)}{Sn(\mu mol/L) + Fe(\mu mol/L)} \times 100 = \frac{2.019}{2.019 + 113.996} \times 100 = 1$$

For $H\text{-}Sn\text{-}Fe_2O_3$,

$$Sn(Atomic\%) = \frac{Sn(\mu mol/L)}{Sn(\mu mol/L) + Fe(\mu mol/L)} \times 100 = \frac{2.11835}{2.11835 + 105.441} \times 100$$

Table S2 Photoelectrochemical activities of Sn-doped and/or Oxygen-deficient hematite reported in literature.

Structure of electrodes	Modification	Technique	Photocurrent at 1.23/1.6 V_{RHE} (mA cm^{-2})	Ref
Mesoporous	Ti and Sn co-doping	In-situ doping of Ti and high-temperature annealing	1.4/2.8	1
Nanorods	Sn doping	Surface treatment of Sn and high-temperature annealing	2.25/-	2
Nanoparticles	Sn doping	Surface treatment and high-temperature annealing	1.1/-	3
Mesoporous	Sn doping	In-situ doping	0.2/0.6	4
Nanorods	Sn doping	High-temperature annealing	0.8/1.1	5
Nanorods	Sn doping	High-temperature annealing	1.4/2.5	6
Nanorods	Sn doping and oxygen deficient	High-temperature annealing in air+N_2	1.5/4.0	7
Nanorod	Sn doping and oxygen deficient	High-temperature annealing in N_2	0.5/0.9	8
Nanoflake	Oxygen deficient	Aerosol-assisted chemical vapor deposition	0.3/1.2	9
Mesoporous	Sn and oxygen deficient	In-situ doping and annealing in H_2	1.0/4.6	this study

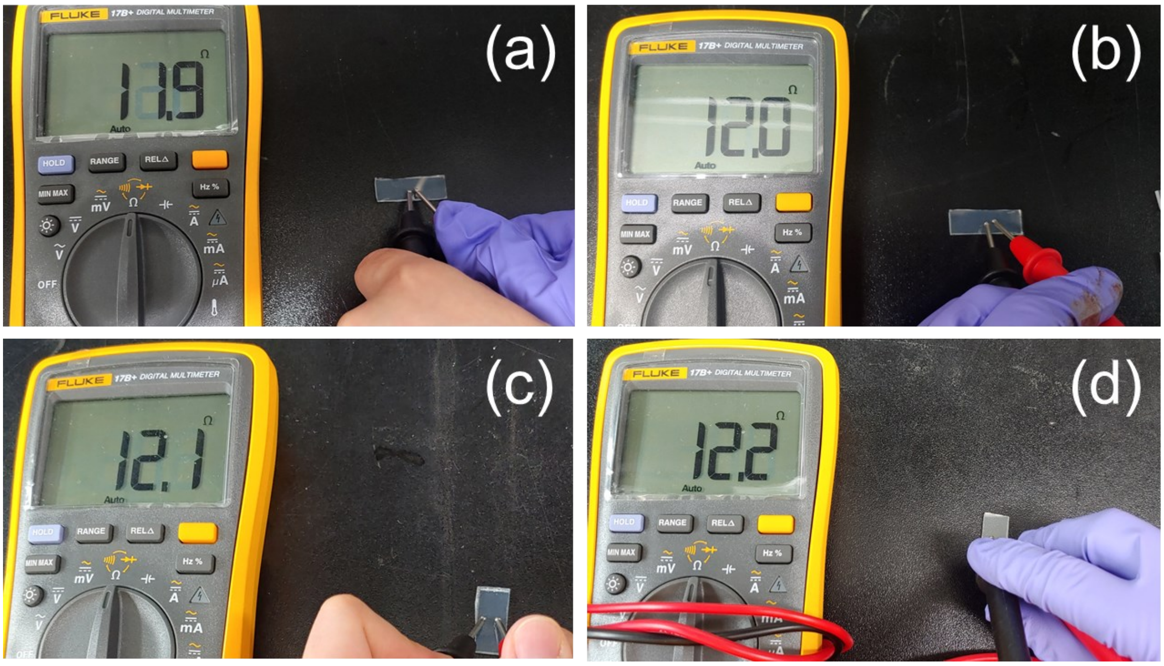

Fig. S1 The resistance of FTO glass (a) before and (b) after H_2 treatment (350 °C for 30 min), and (c) before and (d) after Ar treatment (350 °C for 30 min).

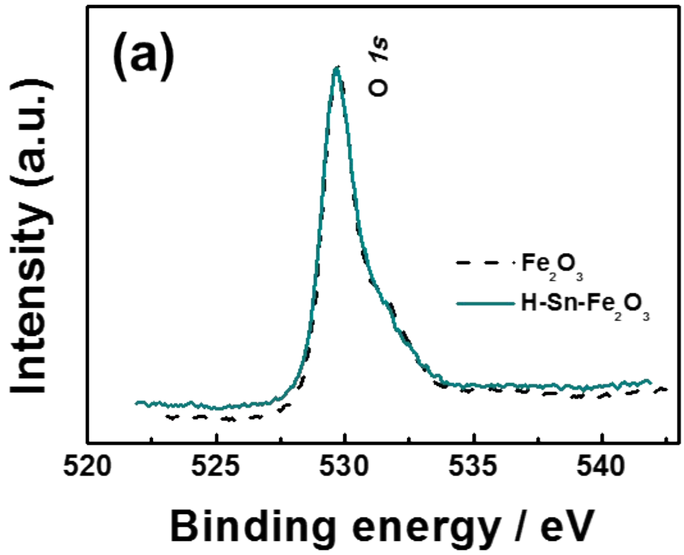

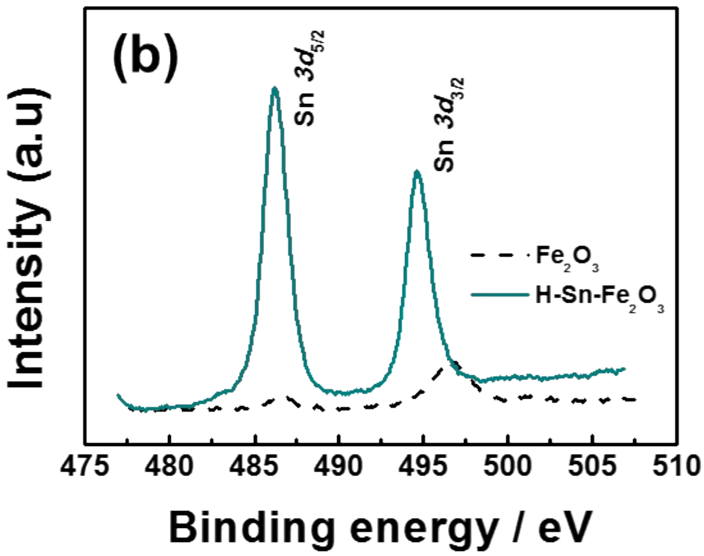

Fig. S2 XPS ((a) O *1s* and (b) Sn *5d*) spectra of bare Fe_2O_3 and H(350 °C)-Sn(8%)-Fe_2O_3.

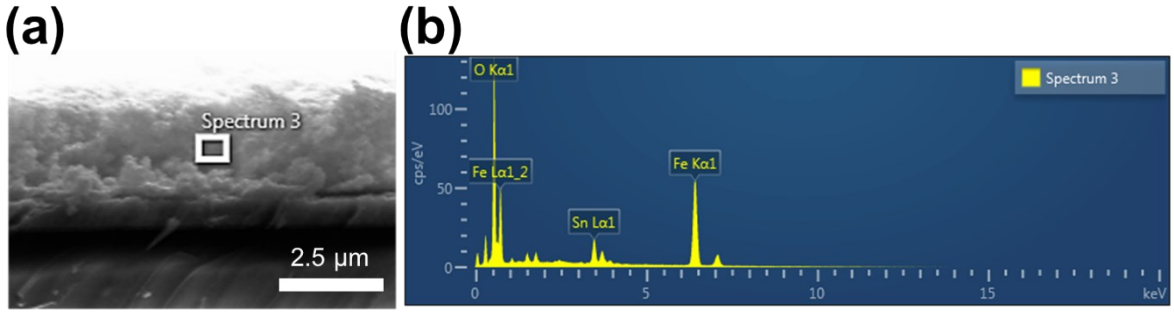

Element	Line Type	Apparent Conc.	K Ratio	Wt%	Wt% Sigma	Atomic %	Standard Label	Factory Standard
O	K series	46.86	0.16	35.28	0.23	67.92	SiO_2	Yes
Fe	K series	43.56	0.44	52.35	0.25	28.87	Fe	Yes
Sn	L series	9.30	0.09	12.37	0.19	3.21	Sn	Yes
Total:				100.00		100.00		

Fig. S3 EDS of cross-sectional view of H(350 °C)-Sn(8%)-Fe_2O_3 from HR-SEM. Atomic% of Sn in H(350 °C)-Sn(8%)-Fe_2O_3 was estimated as followed:

$$Sn(Atomic\%) = \frac{Sn}{Sn + Fe} \times 100 = \frac{3.21}{3.21 + 28.87} \times 100 = 10.006$$

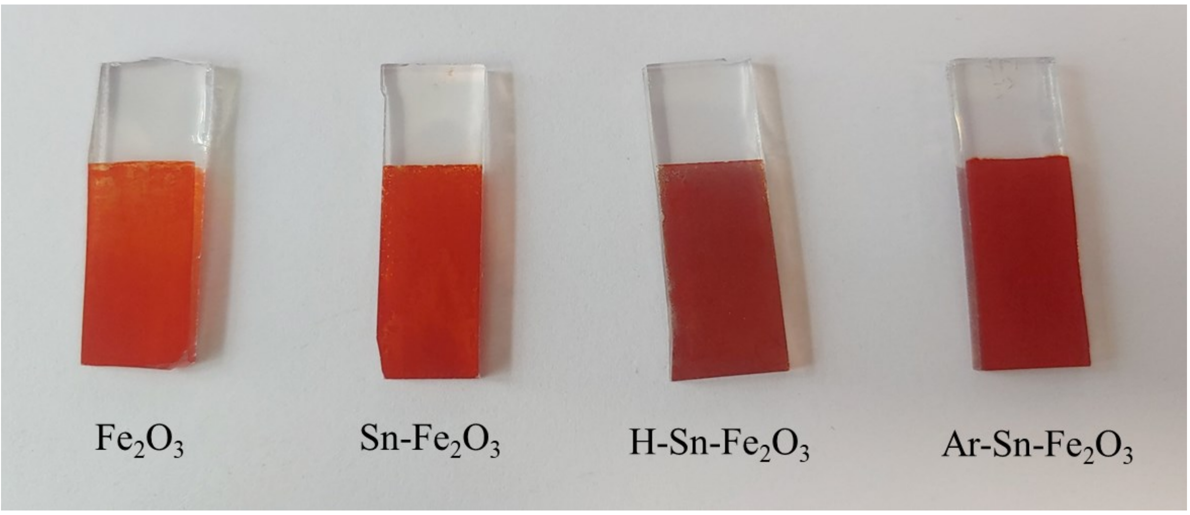

Fig. S4 A photo showing bare and modified Fe_2O_3

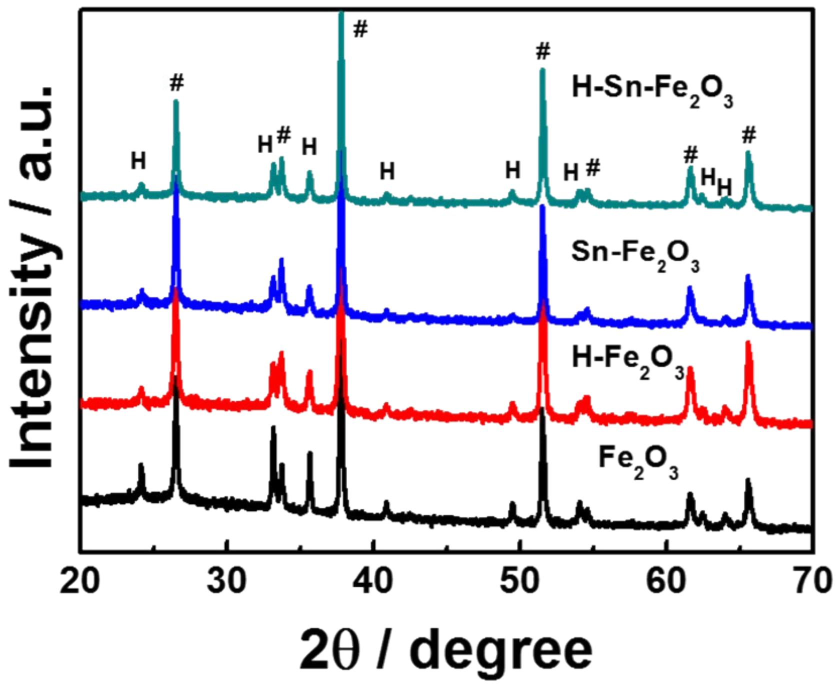

Fig. S5 XRD patterns of bare Fe_2O_3, H-Fe_2O_3, Sn(8%)-Fe_2O_3, and H-Sn(8%)-Fe_2O_3. H and # represent hematite and tin oxide diffraction peaks, respectively. XRD spectra were normalized by Tin oxide peaks of FTO.

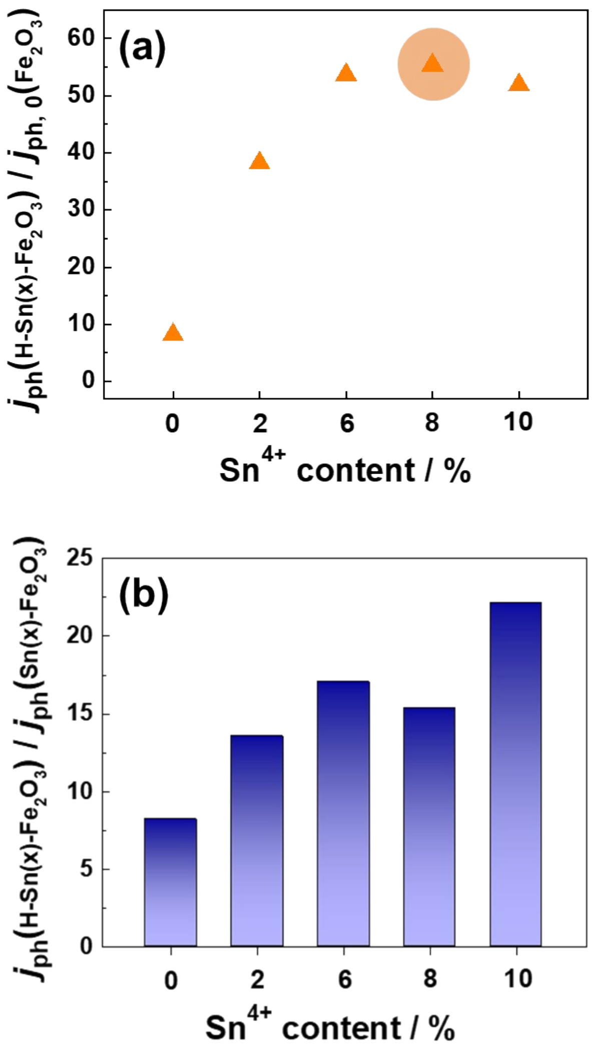

Fig. S6 Photocurrent improvements (a) from Fe_2O_3 to H(350 °C)-Sn(x)-Fe_2O_3 and (b) from Sn(x)-Fe_2O_3 to H(350 °C)-Sn(x)-Fe_2O_3 as a function of initial dopant (Sn^{4+}) concentration. All photocurrent values were obtained from continuous LSV at an applied potential +1.6 V_{RHE}. The experimental conditions were as follows: 1 M KOH, Ar purging, simulated solar light (AM 1.5, 100 mW cm^{-2}).

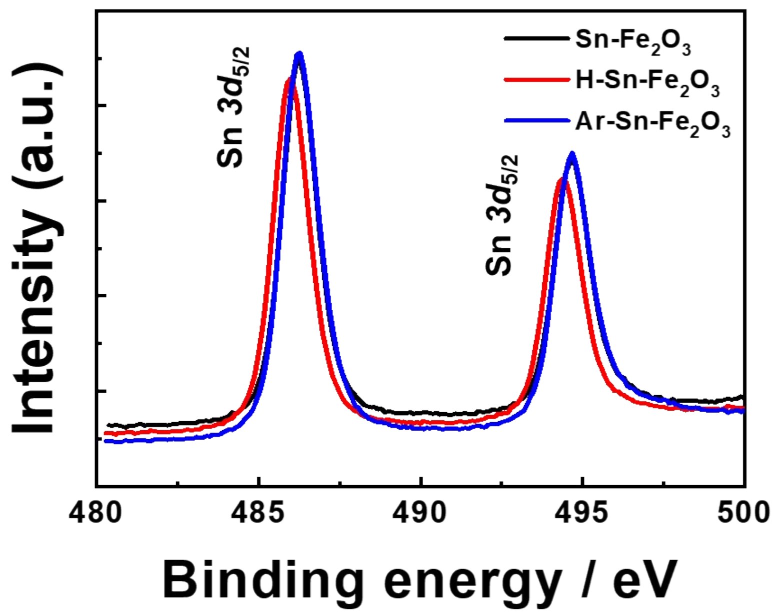

Fig. S7 XPS Sn *3d* spectra of Sn(8%)-Fe_2O_3, H(350 °C)-Sn(8%)-Fe_2O_3, and Ar(350 °C)-Sn(8%)-Fe_2O_3.

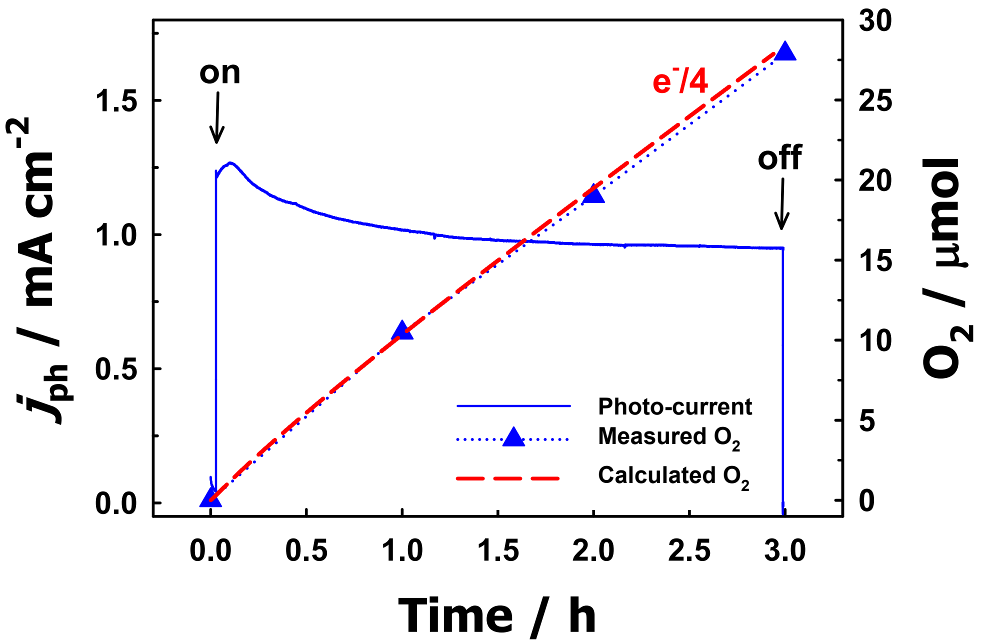

Fig. S8 Photocurrent transients and concurrent oxygen evolution from water oxidation on the Co^{2+}-treated H(350 °C)-Sn(8%)-Fe_2O_3 electrode and at an applied potential of 1.23 V_{RHE} under light illumination (AM 1.5, 100 mW cm^{-2}). The experimental conditions were as follows: 1 M KOH, Ar purging.

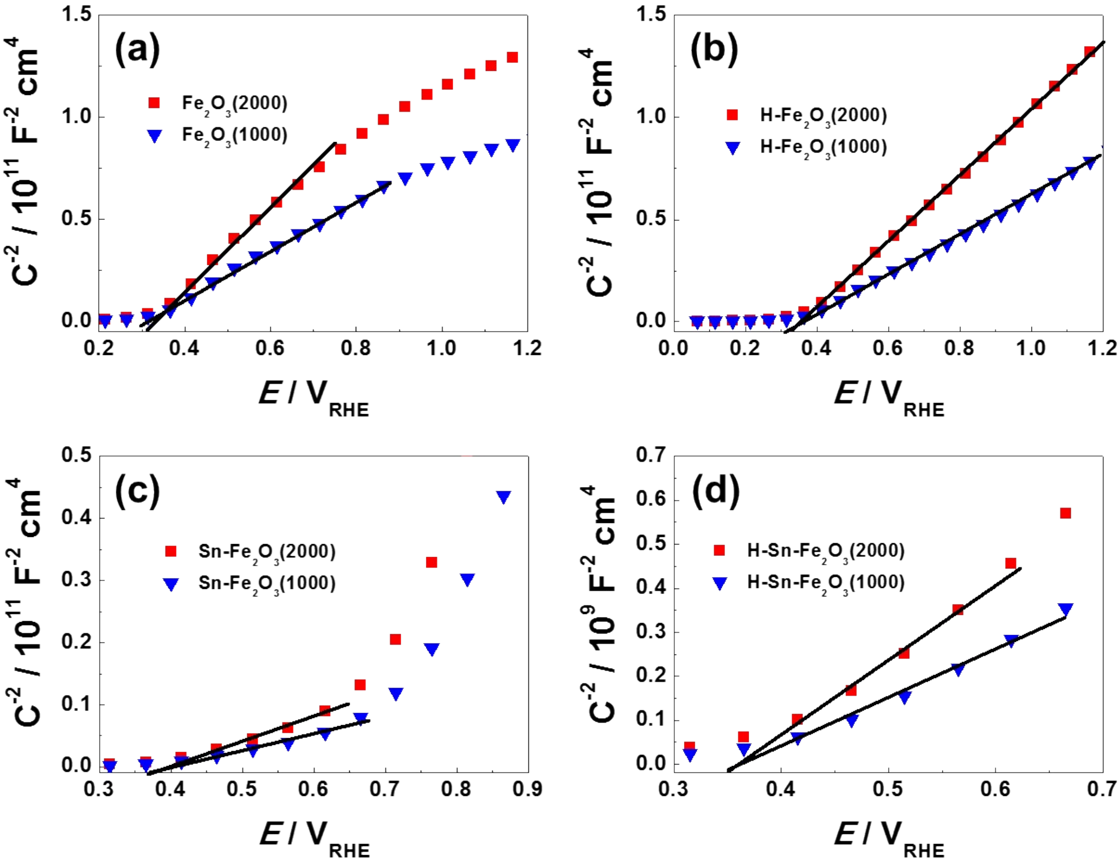

Fig. S9 Mott-Schottky plots of (a) Fe_2O_3, (b) H(350 °C)-Fe_2O_3, (c) Sn(8%)-Fe_2O_3, and (d) H(350 °C)-Sn(8%)-Fe_2O_3 under different frequencies (1 kHz and 2 kHz).

All PEC measurements were conducted versus Ag/AgCl electrode potential and then converted to the reversible hydrogen potential. The reversible hydrogen electrode (RHE) potential was converted from the Ag/AgCl reference potential according to the Nernst equation:[10]

$$E_{RHE} = E_{Ag/AgCl} + 0.059pH + E^0_{Ag/AgCl} \quad (1)$$

where E_{RHE} is the converted potential vs. RHE, $E_{Ag/AgCl}$ is the experimentally measured potential with Ag/AgCl reference electrode, and $E^0_{Ag/AgCl}$ is the potential difference between Ag/AgCl and RHE reference electrodes ($E^0_{Ag/AgCl} \approx 0.1976$ V at 25 °C).

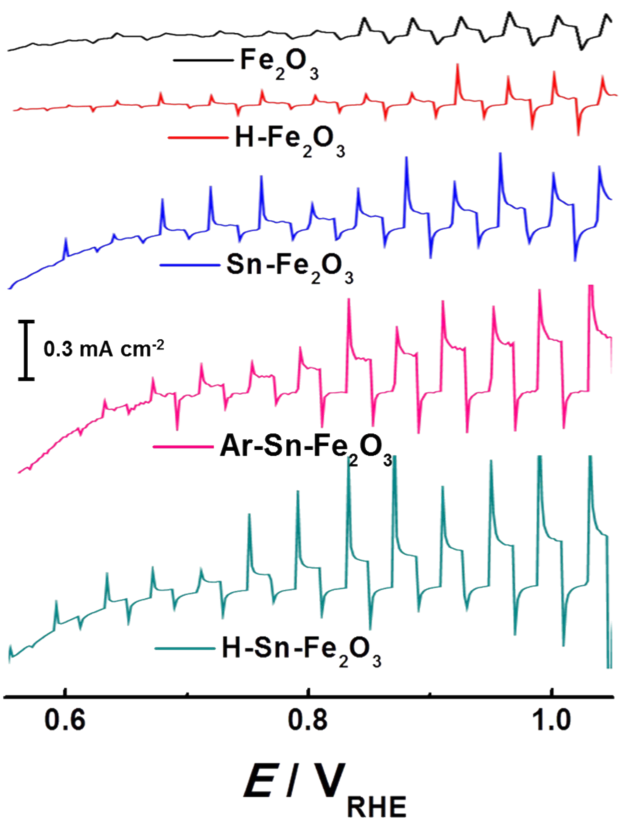

Fig. S10 Linear sweep voltammetry of bare Fe_2O_3, H-Fe_2O_3, Sn(8%)-Fe_2O_3, Ar-Sn(8%)-Fe_2O_3, and H-Sn(8%)-Fe_2O_3 under chopped simulated AM 1.5 illumination with an intensity of 100 mW/cm^2. Electrolyte: 1 M KOH, Ar purged. Scan rate: 20 mV/s for linear sweep voltammetry.

REFERENCES

1. L. Wang, C.-Y. Lee and P. Schmuki, *Electrochem. Commun.*, 2013, 30, 21-25.
2. L. Xi, S. Y. Chiam, W. F. Mak, P. D. Tran, J. Barber, S. C. J. Loo and L. H. Wong, *Chem. Sci.*, 2013, 4, 164.
3. X. Zong, S. Thaweesak, H. Xu, Z. Xing, J. Zou, G. Lua and L. Wang, *Phys. Chem. Chem. Phys.*, 2013, 15, 12314.
4. T. H. Jeon, A. D. Bokarea, D. S. Han, A. Abdel-Wahab, H. Park and W. Choi, *Appl. Catal. B*, 2017, 201, 591-599.
5. C. Tang, B. Sun, M. Li, J. Zhang, X. Fan, F. Gao, Y. Tong, L. Dong and Y. Li, *J. Mater. Chem. A*, 2019, 7, 8050.
6. M. Li, Y. Yang, Y. Ling, W. Qiu, F. Wang, T. Liu, Y. Song, X. Liu, P. Fang, Y. Tong and Y. Li, *Nano Lett*. 2017, 17, 2490-2495.
7. Y. Ling, G. Wang, J. Reddy, C. Wang, J. Z. Zhang and Yat Li, Angew. Chem. Int. Ed. 2012, 51, 4074-4079.
8. A. L.M. Freitas, W. M. Carvalho Jr. and F. L. Souzaa, *J. Mater. Res.*, 2015, 30, 23.
9. M. F. M. Noh, H. Ullah, N. A. Arzaee, A. A. Halim, M. A. F. A. Rahim, N. A. Mohamed, J. Safaei, S. N. F. M. Nasir, G. Wang and M. A. M. Teridi, *Dalton Trans.*, 2020, 49, 12037.
10. G. M. Wang, Y. C. Ling, D. A. Wheeler, K. E. N. George, K. Horsley, C. Heske, J. Z. Zhang and Y. Li, *Nano Letters*, 2011, 11, 3503-3509.